PROCEEDINGS OF SPIE

Scaling and readiness of underlayers for high-NA EUV lithography

Roberto Fallica, Danilo De Simone, Steven Chen, Muhammad Safdar, Hyo Seon Suh

SPIE.

Scaling and readiness of underlayers for high-NA EUV lithography

Roberto Fallica,[a,*] Danilo De Simone,[a] Steven Chen,[a,b] Muhammad Safdar,[a,c] Hyo Seon Suh[a]

[a] IMEC, Leuven, Belgium
[b] Karlsruhe Institute of Technology (KIT), Karlsruhe, Germany
[c] Munich University of Applied Sciences (MUAS), Munich, Germany

ABSTRACT

With the introduction of high-numerical aperture extreme ultraviolet lithography, the thickness of layers in the lithographic stack will scale owing to reduced depth of focus and etch budget. While several studies have explored the impact of thickness scaling on photoresists, the consequence of thinning down underlayers for extreme ultraviolet (EUV) lithography has been scarcely investigated. In this work we assessed the readiness of nine state-of-the-art underlayers, spin-on and dry deposited, scaled in thickness series down to 4 nm nominal (~3 nm actual). Dose-to-size and exposure latitude changed by less than 5 % when thickness of underlayer was decreased. In summary, most of EUV underlayers investigated in this work showed minimal impact on the physical and chemical properties as well as the patterning performance when scaling in view of high numerical aperture extreme ultraviolet lithography.

Keywords: EUV, EUVL, high-NA, underlayer, photoresist, scaling, NA, lithography

1. INTRODUCTION

Extreme ultraviolet (EUV) lithography, the next generation optical lithography technology that uses light at 13.5 nm wavelength, has reached maturity and is being adopted for high volume manufacturing of semiconductor devices worldwide.[1] Currently, commercial EUV scanner models NXE3xxx are equipped with 0.33 numerical aperture (NA) optics that can pattern dense lines/spaces arrays to a resolution of pitch 28 nm. To push forward the resolution towards next technology nodes and reach 20 nm pitch resolution and beyond, a new generation of scanners (EXE5xxx) featuring 0.55 NA is being developed.[2] High-numerical aperture (high-NA) EUV will enable further scaling of integrated circuits by ensuring that the normalized image log-slope (NILS), a metric for the quality of the aerial image,[3] remains at acceptable levels to pattern devices at technology node "2.1nm" and beyond.[4]

From the materials standpoint, photoresists for EUV are expected to fulfill a multitude of requirements such as: high resolution, high sensitivity, low sidewall roughness, low defectivity, thermodynamic stability, high chemical uniformity, and others[5]. The introduction of high-NA EUV will exacerbate these requirements for two reasons. Firstly, the optical depth of focus (DOF) is going to shrink with the reciprocal of the square of numerical aperture according to the well-known equation: $DOF = k_2 \frac{\lambda}{NA^2}$. As a result, the available DOF of a high-NA EUV system will only be about 36% of that of a 0.33 NA scanner, all other parameters being equal. In practice, available depth of focus might reduce from ~ 150 nm[6] to ~ 50 nm thus demanding photoresist thickness reduction (although recent experiments carried out at pseudo-0.5 NA EUV tool showed that the impact might be marginal for contact hole patterning[7]).

The second issue is the need for isotropic scaling in order to maintain a constant aspect ratio when pitch shrinks. This problem is not specific to high-NA EUV: when pitch shrinks, aspect ratio of photoresist patterns increases which in turn leads to higher collapse probability during development and rinse[8]. To mitigate pattern collapse, photoresists for high-NA EUV will have to be thinner than those used today with detrimental consequences on the local critical dimension uniformity, line edge/width roughness (LER/LWR), process window[9], and on signal-to-noise ratio of scanning electron microscopy (SEM) image acquisition[10] and data extraction[11]. Consequently, great effort is being put into investigating and predicting thin photoresist films performance ahead of high-NA EUV. A variety of new approaches such as etch-litho

---

* roberto.fallica@imec.be; imec-int.com

synergy[9], pre- and post-processing holistic approach[12], photoresist-underlayer matching[8], complementary direct self-assembly[13], and others, are being taken to this purpose.

Meanwhile, it should not be overlooked that underlayers (a.k.a. hardmasks) also have to scale in thickness due to etching budget considerations. Take for instance the positive-tone chemically amplified resists (CAR), typically between 35 and 45 nm thick, used nowadays for pitch 32 nm lines/spaces patterning: several technology nodes ahead, the 16 nm pitch lines/space will have to use 20 nm thick photoresists to maintain the same aspect ratio as today. Underlayers will arguably have to shrink at a comparable rate, from 10 nm of today to 4 or 3 nm foreseen in technology node "2.1nm" (under the assumption that etch selectivity of photoresist vs. underlayer remains the same). These estimates lead to the qualitative scaling roadmap shown in Fig. 1.
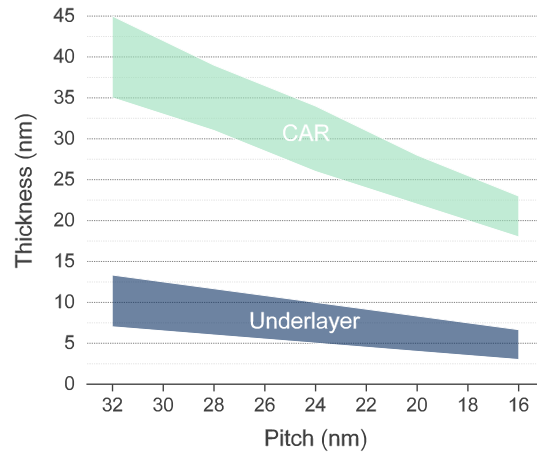

Figure 1. A qualitative roadmap of photoresists and underlayers thickness scaling in EUV lithography. For photoresist we consider here only positive-tone CAR. Photoresist thickness ranges between 35 and 45 nm at pitch 32 nm lines/spaces patterning and, for pattern collapse reasons, is expected to shrink to 20 nm in future technology nodes. The underlayer thickness is typically 10 nm as of today and is expected to follow a comparable scaling trend.

Despite these considerations, the scaling effects on EUV underlayers have not been explored as extensively as those on photoresists. A number of physical and chemical properties of thin films are have been demonstrated to vary with thickness at the nanoscale, such as: glass transition temperature[14], elastic modulus[15], surface roughness[16], [17], correlation length[17], Hurst's exponent[16], refractive index[18], and radius of gyration[19], as well as theoretically[20]. Any such change is evidently undesirable from lithographic process control standpoint and is relevant for EUV lithography as witnessed by early works that studied the glass transition temperature as a function of thickness[21], and recent characterization of EUV underlayers scaled down to 5 nm[22].

For all these reasons, in this work we evaluated the readiness of underlayer scaling for high-NA EUV lithography from the point of view of their physical properties and impact on patterning quality. In collaboration with external materials suppliers, we had the opportunity to characterize nine underlayer samples in thickness series down to 4 nm (nominal thickness) so as to replicate the process conditions foreseen in future technology nodes. Potential roadblocks include thickness uniformity, density fluctuations and uneven coverage. In the second part we look at the lithographic impact of thinning underlayers by EUV patterning of a state-of-art chemically amplified resist.

2. SAMPLES DESCRIPTION AND EXPERIMENTAL DETAILS

2.1 Samples description: the photoresist and the underlayers

In this study, four materials suppliers provided nine underlayers (UL) and one chemically amplified resist (CAR), all specifically designed for EUV lithography. The nine underlayers' chemistry varied and included siloxanes,

polycarbosilanes, silicon oxycarbide glasses, and others. A organic underlayer (B) was also measured as benchmark. The CAR, positive tone organic resist, 30 nm thick was preliminarily qualified for pitch 28 nm EUV patterning capability on a reference underlayer (data not reported). Spin-coated samples were prepared in 300 mm track; deposited samples were prepared in proprietary 300 mm-scale deposition tools. Materials suppliers were required to provide underlayers in series of at least two thickness versions each, with a target of 5 to 3 nm minimum nominal thickness. There was no other specific requirement for the underlayer typology. Notably, materials suppliers were also informed that the photoresist of choice was organic CAR, and it was intended that the underlayer should be suited and optimized for this specific case. Care was taken to follow the manufacturers' specifications to maximize quality and yield of the samples. The underlayers were coated or deposited directly on top of bare silicon wafers of 300 mm diameter and 775 µm thickness. These wafers typically have a native Si oxide layer. The underlayers codenames and nominal thickness are summarized in Table 1.

Table 1. Samples description: underlayers codename and their nominal thickness, and photoresist used and its thickness.

Underlayer codename	Thickness, nominal (nm)
A	8, 6, 4
B	20, 5
C	8, 6, 4
D	8, 6, 4
E	8, 6, 4
F	8, 6, 4
G	8, 6, 4
H	8, 6, 4
L	10, 5
Photoresist	**Thickness, nominal (nm)**
Positive tone CAR	30

2.2 Physical characterization methods

Experimental characterization was carried out on blanket underlayers films (unpatterned and not covered with photoresist) to validate actual thickness, thickness uniformity across 300 mm wafer, and surface roughness. To get an as accurate as possible measurement of the actual thickness of the ultrathin underlayer samples, X-ray reflectivity was used (Cu Kα source, 0.154 nm wavelength). A 300 mm-scale spectroscopic ellipsometer in the wavelength range 215-800 nm was used to determine the standard variation of the film thickness across 21 measurement locations on wafer. Together, these two techniques are complementary. It should be noted that native silicon oxide layer (between 1 and 2 nm thick)[23], [24] is ubiquitously present on bare <100> Si surface and is a source of measurement error especially when the underlayer also contains Si, O, or Si-O bonds.

2.3 EUV lithography

Assessment of thin underlayers' impact on CAR lithography was performed using ASML's NXE3400B EUV scanner located at IMEC (Leuven, Belgium) premises. An EUV reticle featuring dense vertical lines/spaces arrays of pitch 28 nm and nominal 1:1 ratio was used to pattern the wafer in a focus-exposure-matrix (FEM) fashion. The center dose of the FEM wafers was 67 mJ/cm^2, the dose step was 1.5 mJ/cm^2, the center focus was 0.000 µm, and the focus step was 0.020 µm. The EUV illuminator was a customized X dipole specifically optimized for pitch 28 nm dense vertical lines/spaces.

2.4 CDSEM inspection after lithography and computational metrology

Photoresist samples were inspected after EUV exposure and development by critical dimension scanning electron microscope (CDSEM) with field of view of 0.82^2 µm^2 and 0.8 nm/pixel resolution. Lines' critical dimension (CD) measured on focus-exposure matrix wafers were used to calculate dose-to-size (at CD = pitch/2), best focus, and elliptical exposure latitude (as CD = pitch/2 ± 10 %). For each wafer, the chip that was closest to the calculated dose-to-size and

best focus was then inspected in depth by taking 50 CDSEM images with field of view 1.6^2 µm^2 and 0.8 nm/pixel resolution according to previously defined protocol[25]. These 50 images were analyzed as a batch using FRACTILIA's MetroLER software (v. 2.8.5)[26] to determine unbiased line width roughness (LWR), unbiased line edge roughness (LER), power spectral density (PSD), correlation length, and PSD(0), according to well-established methodology.[27]

3. RESULTS

3.1 Quality of blanket scaled underlayers

Initial assessment of underlayers quality involved the characterization of the blanket films to determine the materials' coverage of the wafer. The actual measured underlayer thickness (symbols in Fig. 2) was in most cases below target by about 1 nm and occasionally, such as underlayers (A), as much as 2 nm below target. Some underlayers (E, F, G) showed an approximately constant offset with respect to the target thickness which might be ascribed to a systematic measurement error due to the presence of native silicon oxide. In one case, thickness accuracy was better in the thinner version than it was for the thicker, which led to a narrower thickness range (D). In another case (C), this trend was reversed, which led to a broader thickness spread. The thickness uniformity, across 21 measurement locations on the 300 mm wafer, is reported as the error bar in Fig. 2. Uniformity varied greatly from high (A, L) to low (D) and is ascribed to underlayer preparation methods, which included manual coating by pipette, coating from small volume dispenser units, track coating from gallon supply, and dry deposition. It should be noted that thickness targeting was not the main scope of this work and does not invalidate our methodology, as long as samples with well-defined thickness series can be accurately obtained.
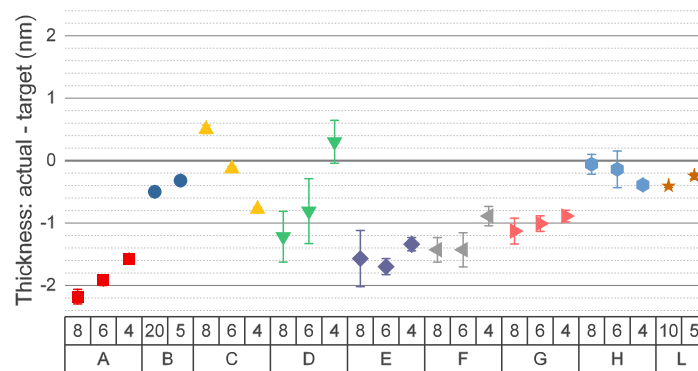

Figure 2. Difference between actual thickness and target thickness, in nm, of the blanket underlayers. In the X-axis, letters are codenames for underlayers; numbers indicate the target nominal thickness. Symbols represent thickness measured by XRR; error bars indicate coating uniformity across 21 locations on a 300 mm wafer by ellipsometry.

3.2 EUV lithography performance on scaled underlayers

In this section we review the impact of reducing underlayers thickness on the lithographic performance of a chemically amplified resist. Dose-to-size, depth of focus, exposure latitude, linewidth roughness, failure free process window, and Z-factor[28] are the key performance indicators used. To focus on the relative variations of the key parameters with thickness, all data reported here was normalized to the thickest layer of each underlayer type.

The CDSEM images of CAR patterned on the nine underlayers in thickness series, 25 samples in total, taken at the chip closest to dose-to-size and best focus of the FEM wafer, are shown in Fig. 3. It can be noted that image contrast varies among these samples, something we mainly ascribe to different secondary electron yield of each underlayer type. Within each thickness series, contrast also changes, although to a lesser extent than it has been reported in the case of thin photoresist films[10]. CAR patterning does not show any problem at the dose-to-size and best focus when used in conjunction with most of these underlayers. One underlayer (H) showed mediocre adhesion and pattern collapse possibly due to mismatching surface energy with photoresist. Adhesion of (H) seemed to improve when thinner version was used (H4), for reasons unclear.
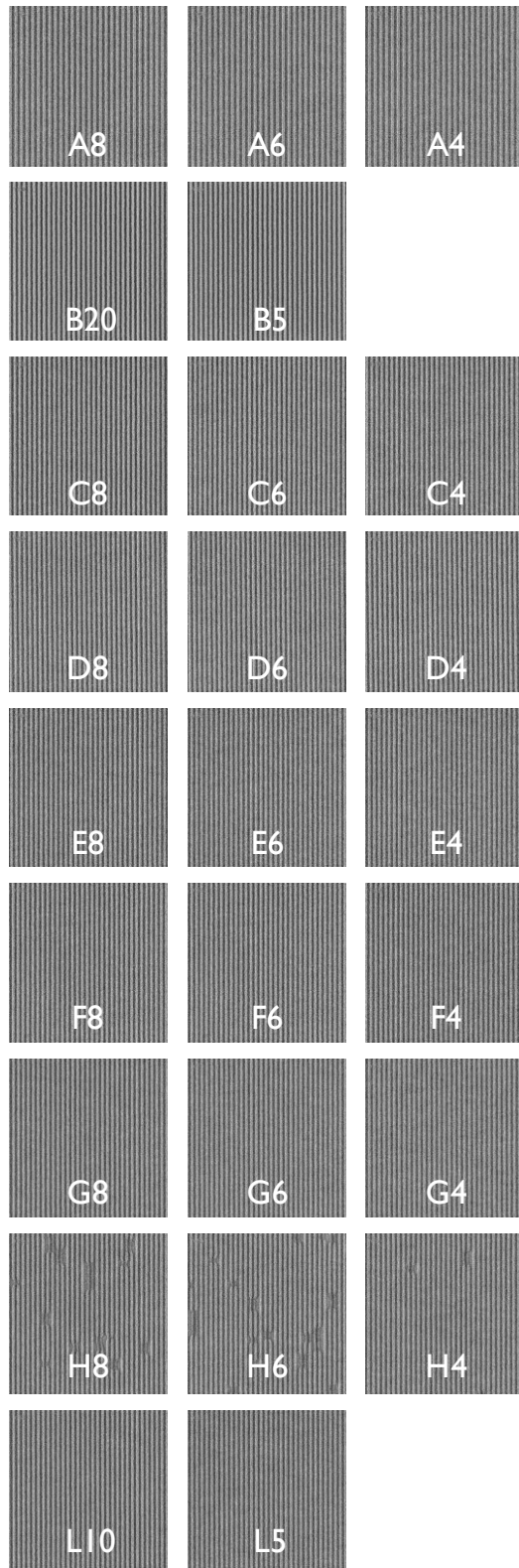
Figure 3. CDSEM images of CAR lines/spaces patterns of pitch 28 nm, printed on nine underlayers of decreasing thickness. The letter indicates the underlayer sample, the number indicates the nominal underlayer thickness, in nm.

The relative effect of underlayer thickness on dose-to-size is summarized in Fig. 4, where data is again normalized to the dose-to-size of the thickest layer of each type. The effect of underlayer thickness on dose-to-size was less than ± 3 %, which is nearly within experimental and reproducibility error. Similar considerations could be done for the exposure latitude, calculated by elliptical process window, and shown in relative terms in Fig. 5. EL was minimally impacted by thickness scaling (< ± 5%) for most of the samples, with the exception of (C) which had an EL reduction of -12 % at worst.
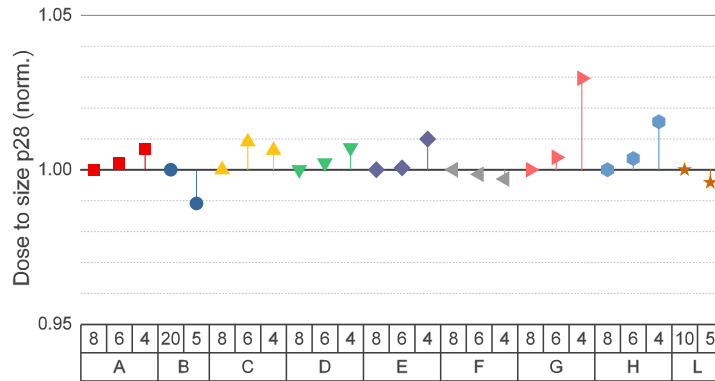

Figure 4. Dose-to-size of a CAR, pitch 28 nm lines/spaces, patterned by EUV on top of nine different underlayers of decreasing thickness. Values are normalized to the dose-to-size of the thickest film of each type. Effect of underlayer thickness on dose-to-size was below ± 3 %.
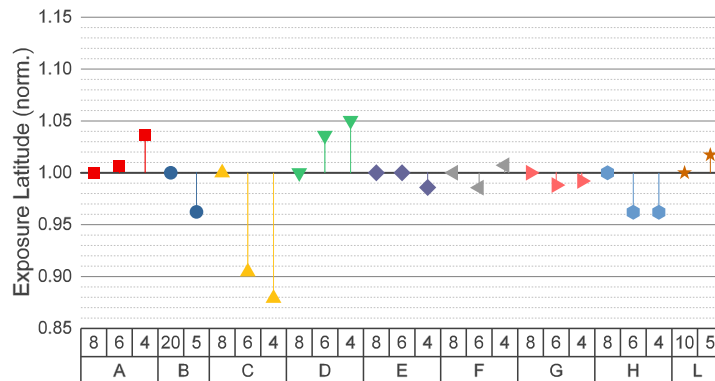

Figure 5. Exposure latitude of a CAR, pitch 28 nm lines/spaces, patterned by EUV on top of nine different underlayers of decreasing thickness and calculated by elliptical process window. Values are normalized to the exposure latitude of the thickest film of each type. Effect of underlayer thickness on exposure latitude was below ± 5 % for most underlayers.

In a follow-up study we will explore the effect of underlayer thickness on the linewidth roughness. Preliminary evidence shows that the high frequency component of the LWR will be impacted by scaling underlayer thickness. Moreover, the global photoresist performance will be evaluated by the Z-factor to indicate the impact of underlayer type and thickness. Thickness reduction and confinement at the nanoscale can impact the surface of underlayer as well, which should be explored by analyzing the power spectral density of the surface of the underlayer, a methodology not yet developed.

4. CONCLUSIONS

Underlayers for high-NA EUV will likely be scaled down in thickness so as to meet the requirements of shallow depth of focus and etch budget. Owing to the imminent transition to high-NA EUV systems, assessment of underlayers is a

technologically crucial topic, although neglected so far. In this work we studied nine underlayer types produced in thickness series, down to 4 nm nominal (~ 3 nm actual thickness). Materials properties (thickness, uniformity, surface roughness, and surface energy) were assessed on blanket films. EUV lithography was performed using a positive tone CAR. The sensitivity, process latitude indicated that underlayer thickness had a very limited impact on lithography performance. Interestingly, lithography performance is more sensitive to underlayer type than thickness: in other words, when CAR performed poorly, it did so regardless of underlayer thickness which indicates that the matching between photoresist and underlayer is the major effect to look for when optimizing underlayers.

ACKNOWLEDGEMENTS

REFERENCES

[1] C. Smeets *et al.*, "0.33 NA EUV systems for high-volume manufacturing," in *Optical and EUV Nanolithography XXXV*, 2022, vol. PC12051. doi: 10.1117/12.2614220.

[2] J. Van Schoot *et al.*, "High-NA EUV lithography exposure tool: advantages and program progress," in *Extreme Ultraviolet Lithography 2020*, Online Only, United States, Jan. 2021, p. 35. doi: 10.1117/12.2572932.

[3] C. A. Mack, *Fundamental principles of optical lithography: the science of microfabrication*. Chichester, West Sussex, England ; Hoboken, NJ, USA: Wiley, 2007.

[4] M. Neisser *et al.*, "Lithography," in *2021 IEEE International Roadmap for Devices and Systems Outbriefs*, Santa Clara, CA, USA, Nov. 2021, pp. 1–11. doi: 10.1109/IRDS54852.2021.00017.

[5] A. Robinson and R. Lawson, Eds., *Materials and processes for next generation lithography*. Amsterdam: Elsevier, 2016.

[6] D. De Simone *et al.*, "EUV photoresist patterning characterization for imec N7/N5 technology," in *Extreme Ultraviolet (EUV) Lithography IX*, San Jose, United States, Mar. 2018, p. 12. doi: 10.1117/12.2299504.

[7] J. Santaclara *et al.*, "Resist and reticle activities towards High-NA EUV ecosystem readiness," in *Optical and EUV Nanolithography XXXV*, San Jose, United States, Jun. 2022, p. 7. doi: 10.1117/12.2614162.

[8] R. Fallica, S. Chen, D. De Simone, and H. S. Suh, "Adhesion and collapse of extreme ultraviolet photoresists and the role of underlayers," *J. Micro/Nanopattern. Mats. Metro.*, vol. 21, no. 03, Jul. 2022, doi: 10.1117/1.JMM.21.3.034601.

[9] D. De Simone *et al.*, "A lithographic and etching study on EUV contact hole patterning for stochastic process mitigation towards advanced device scaling," in *Optical and EUV Nanolithography XXXV*, San Jose, United States, Jun. 2022, p. 44. doi: 10.1117/12.2614165.

[10] G. F. Lorusso *et al.*, "Metrology of thin resist for high NA EUVL," in *Metrology, Inspection, and Process Control XXXVI*, San Jose, United States, May 2022, p. 2. doi: 10.1117/12.2614046.

[11] C. A. Mack, J. Severi, M. Zidan, D. De Simone, and G. F. Lorusso, "Unbiased roughness measurements from low signal-to-noise ratio SEM images," in *Metrology, Inspection, and Process Control XXXVI*, San Jose, United States, May 2022, p. 64. doi: 10.1117/12.2614454.

[12] A. Raley *et al.*, "Outlook for high-NA EUV patterning: a holistic patterning approach to address upcoming challenges," in *Advanced Etch Technology and Process Integration for Nanopatterning XI*, San Jose, United States, May 2022, p. 18. doi: 10.1117/12.2613063.

[13] H. S. Suh *et al.*, "Exploring the synergy between EUV lithography and directed self-assembly," in *Novel Patterning Technologies 2022*, San Jose, United States, Jun. 2022, p. 8. doi: 10.1117/12.2622565.

[14] C. B. Roth, "Polymers under nanoconfinement: where are we now in understanding local property changes?," *Chem. Soc. Rev.*, vol. 50, no. 14, pp. 8050–8066, 2021, doi: 10.1039/D1CS00054C.

[15] J. M. Torres, C. M. Stafford, and B. D. Vogt, "Elastic Modulus of Amorphous Polymer Thin Films: Relationship to the Glass Transition Temperature," *ACS Nano*, vol. 3, no. 9, pp. 2677–2685, Sep. 2009, doi: 10.1021/nn9006847.

[16] F. Elsholz, E. Schöll, and A. Rosenfeld, "Control of surface roughness in amorphous thin-film growth," *Appl. Phys. Lett.*, vol. 84, no. 21, pp. 4167–4169, May 2004, doi: 10.1063/1.1755425.

[17] T. Gredig, E. A. Silverstein, and M. P. Byrne, "Height-Height Correlation Function to Determine Grain Size in Iron Phthalocyanine Thin Films," *J. Phys.: Conf. Ser.*, vol. 417, p. 012069, Mar. 2013, doi: 10.1088/1742-6596/417/1/012069.

[18] Y. Han, X. Huang, A. C. W. Rohrbach, and C. B. Roth, "Comparing refractive index and density changes with decreasing film thickness in thin supported films across different polymers," *J. Chem. Phys.*, vol. 153, no. 4, p. 044902, Jul. 2020, doi: 10.1063/5.0012423.

[19] P. F. Green, E. Glynos, and B. Frieberg, "Polymer films of nanoscale thickness: linear chain and star-shaped macromolecular architectures," *MRS Communications*, vol. 5, no. 3, pp. 423–434, Sep. 2015, doi: 10.1557/mrc.2015.56.

[20] M. Raible, S. G. Mayr, S. J. Linz, M. Moske, P. Hänggi, and K. Samwer, "Amorphous thin-film growth: Theory compared with experiment," *Europhys. Lett.*, vol. 50, no. 1, pp. 61–67, Apr. 2000, doi: 10.1209/epl/i2000-00235-7.

[21] C. Higgins, S. Kruger, V. Kamineni, R. Matyi, J. Georger, and R. Brainard, "Understanding Ultra-Thin Film Resist and Underlayer Performance through Physical Characterization," *J. Photopol. Sci. Technol.*, vol. 23, no. 5, pp. 699–707, 2010, doi: 10.2494/photopolymer.23.699.

[22] J. H. Sim *et al.*, "Thickness dependence of properties of EUV underlayer thin films," in *Advances in Patterning Materials and Processes XXXIX*, San Jose, United States, May 2022, p. 21. doi: 10.1117/12.2613437.

[23] M. Morita, T. Ohmi, E. Hasegawa, M. Kawakami, and M. Ohwada, "Growth of native oxide on a silicon surface," *Journal of Applied Physics*, vol. 68, no. 3, pp. 1272–1281, Aug. 1990, doi: 10.1063/1.347181.

[24] C. Bohling and W. Sigmund, "Self-Limitation of Native Oxides Explained," *Silicon*, vol. 8, no. 3, pp. 339–343, Jul. 2016, doi: 10.1007/s12633-015-9366-8.

[25] G. F. Lorusso, T. Sutani, V. Rutigliani, F. Van Roey, and A. Moussa, "Need for LWR metrology standardization: the imec roughness protocol," *J. Micro/Nanolith. MEMS MOEMS*, vol. 17, no. 04, p. 1, Sep. 2018, doi: 10.1117/1.JMM.17.4.041009.

[26] C. A. Mack and B. D. Bunday, "Analytical linescan model for SEM metrology," in *Metrology, Inspection, and Process Control for Microlithography XXIX*, 2015, vol. 9424, pp. 117–139. doi: 10.1117/12.2086119.

[27] G. P. Patsis, V. Constantoudis, A. Tserepi, E. Gogolides, G. Grozev, and T. Hoffmann, "Roughness analysis of lithographically produced nanostructures: off-line measurement and scaling analysis," *Microelectronic Engineering*, vol. 67–68, pp. 319–325, Jun. 2003, doi: 10.1016/S0167-9317(03)00085-6.

[28] T. Wallow *et al.*, "Evaluation of EUV resist materials for use at the 32 nm half-pitch node," San Jose, California, USA, Mar. 2008, p. 69211F. doi: 10.1117/12.772943.